Journal of University of Science and Technology Beijing
1995, Vol 2, No 2: 84 ~ 91

COMPUTER SIMULATION OF GRAIN BOUNDARY SEGREGATION BEHAVIOR AND MECHANISMS OF STRENGTHENING OF Mg IN Ni-BASED SUPERALLOYS

CHEN GUOLIANG GE HONGLIN
State Key Laboratery for Advanced Metals and Materials, USTB, Beijing 100083, PRC
(Received 1994-12-12)

ABSTRACT This paper used EAM and static relaxation method to simulate the grain boundary segregation behavior of Mg in Ni-based superalloys. The results offer a better understanding in the strengthening mechanism of Mg addition in superalloys. The segregation of Mg increases the grain boundary cohesive bond and the vacancy formation energy, and decreases the mobility of grain boundary dislocation. It results in the retardation of creep voids initiation and growth.

KEY WORDS Mg in Superalloys, Grain boundary segregation , superalloy , computer simulation

RECENTLY a systematic research on the effects of Mg on Ni-based superalloys has been conducted in China [1]. Our previous studies [2 ~ 4] showed that small addition of Mg in various Ni-based superalloys would significantly improve the stress rupture life and ductility, creep notch sensitivity, high temperature tensile ductility and hot workability. The beneficial effects of Mg in superalloys can be maintained even after 5 000 h long time exposure at high temperature. Many observations have illustated the grain boundary segregation behavior of Mg, and it led to refine the grain boundary precipitates such as carbides. All experimental results have proved that the beneficial effects of Mg are associated with grain boundary behavior , but until recently there has been little detailed information on the mechanism involved.

1 THEORETICAL METHOD

According to the embedded-atom method (EAM) , the total energy for an alloy system can be approximately written:

$$E_{\text{total}} = \sum_i F_i(t_i\rho_i) + 1/2\sum_i \sum_{i \neq j} \Phi t_i t_j(r_{ij}) \quad (1)$$

where ρ_i is the electron density at atom i due to the remain atoms of the system. t_i and t_j are the types of atoms. The electron density ρ_i is approximated by the superposition atomic density:

$$\rho_i = \sum_{j(\neq i)} \rho t_j r_{ij}$$

where $\rho t_j(r_{ij})$ is the electron density contributed by atom t_j. $F_i(t_i\rho_i)$ is the energy embedding atom i into the background electron density ρ_i, and $\Phi(r_{ij})$ is the core-core pair repulsion between atoms i and j separated by the distance r_{ij}. In the case of two different species the core-core pair repulsion term $\Phi_{t_it_j}(r_{ij})$ can be written :

$$\Phi_{t_it_j}(r_{ij}) = \Phi_{t_i}(r_{ij})\Phi_{t_i}(r_{ij})/r_{ij} \quad (2)$$

The effective charge is constrained to be positive and to decrease monotonically with increasing separation.

In order to do the simulation, the segregation behavior of Mg in Ni-based superalloys was simplified to that in pure Ni . In this case all necessary parameters mentioned in previous paragraph can be obtained : $\rho_{Ni}(r)$ and $\rho_{Mg}(r)$ as shown in Fig. 1, which was calculated from the Hartree-Fock wave functions.

The embedding function of Ni, $F_{Ni}(\rho)$ can be obtained by a computer program, which is similar to Foiles work [5].

The pair repulsion term is cited from the same work :

$$\Phi_{Ni}(r) = 10.0(1 + 0.895\ 7r)\exp(1.863\ 3r) \quad (3)$$

Table 1 shows the observed and calculated physical constants for pure Ni. It can be seen they are consistent with each other .

The embedding function of Mg, $F_{Mg}(\rho)$ is cited from Ref. [6], and the pair-repulsion term of Mg can be expressed [7]:

$$\Phi_{Mg}(r) = 3\ 829.0\exp(-3.698\ 13r)$$

Then the pair repulsion term between Ni and Mg atom can be written :

$$\Phi_{NiMg}(r) = [\Phi_{Ni}(r) \cdot \Phi_{Mg}(r)]/r$$

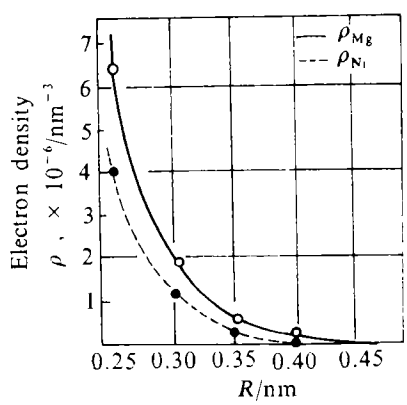

Fig . 1 The electron density ρ as a function of distance R for Ni and Mg

Table 1 Physical constants of pure Ni used to determine the function

Properties	Calculated value	Expermental value
a_0 /nm	0.352	0.352
E_{sub} /eV	4.45	4.45
$B \times 10^{-7}$/J · cm^{-3}	1.81	1.84
$C_{11} \times 10^5$ /J · cm^{-3}	2.33	2.465
$C_{12} \times 10^5$ /J · cm^{-3}	1.54	1.473
$C_{44} \times 10^5$ /J · cm^{-3}	1.28	1.247
E_v/eV	1.63	1.6

The static relaxation method was used: starting from a rigid bicrystal coincidence boundary with protruding atoms removed, the energy was minimized by two steps: first, was the rigid body translation method which often accounts for the major part of the relaxation energy; and second, was the individual displacements of all atoms incrementally and relatively in the direction of the steepiest local energy gradient which continued until the energy minimum was reached. Sutton and Vited's structure unit model was used to describe the grain boundary structure.

Following equations were used for the calculation of the grain boundary energy and the segregation energy:

$$E_{gb} = 1/A[\sum (E_f - E_p)] \tag{6}$$

$$E_{segr} = \Delta E_{gb} - \Delta E_{bulk} \tag{7}$$

where E_{gb} and E_{segr} are the grain boundary energy and segregation energy, respectively. A is the area of the unit cell paralled to the grain boundary face. E_f and E_p are the atomic energies in a body with and without grain boundary respectively. ΔE_{gb} and ΔE_{bulk} are the energy increments in the relaxation condition of the solute locating grain boundary and bulk respectively. When the segregation energy, E_{segr}, is negative the grain boundary segregation is thermodynamic stable.

In order to study the relationship between the grain boundary segregation and grain boundary dislocation, the local stress tensor at grain boundary in terms of hydrostatic stress field was calculated by using the method described in Refs. [8, 9].

The influence of Mg segregation on the vacancy formation energy was also calculated.

2 RESULTS AND DISCUSSION

2.1 CALCULATED FEATURES OF GRAIN BOUNDARY STRUCTURE AND ENERGY

Table 2 summarizes the calculated results in the structures and energies of symmetrical [100] tilt grain boundaries of Ni. It can be seen that despite the interaction potential used in the paper is different from the traditional pair potential approach the calculated grain boundary structures are basically the same from the structure unit point of view [10]. The possible variants of grain boundary structure is also instanced in Table 2. However, the grain boundary energies for different structure variants of a grain boundary are different from each other. For example, the grain boundary energy of |B • B| structure and |B′ • B′| structure for $\Sigma = 5(210)36.87^\circ$ /[001] boundary are $1.501\,9 \times 10^{-4}$ and $1.550\,2 \times 10^{-4}$ J/cm^2, respectively. The structure with minimum boundary energy was selected to study segregation behavior in this paper.

The experimental average energy value of high angle grain boundary at 1060℃ in Ni cited from Ref. [11] is 8.66×10^{-5} J/cm^2. The Ref. [11] also gave a linear temperature dependence of grain boundary energy, therefore the extrapolated average energy value can be estimated to be 1.450×10^{-4} J/cm^2 at 0K. The extrapolated value consists with the calculated data range $1.340 \times 10^{-4} \sim 1.550 \times 10^{-4}$ J/cm^2.

2.2 BASIC GRAIN BOUNDARY SEGREGATION BEHAVIOR OF Mg

Structure unit model of grain boundary provides a way to study the segregation be-

Table 2 Grain boundary structure and energy

Grain boundary plane	θ/(°)	Σ	Structure	Energy/mJ · m^{-2}
$(540)_1/(450)_2$	12.86	41	|AAAB'|	1 340.4
$(320)_1/(230)_2$	22.62	13	|AB'|	1 400.3
$(530)_1/(350)_2$	28.07	17	|ABB'|	1 456.7
$(210)_1/(120)_2$	36.87	5	|B · B|	1 504.9
$(210)_1/(120)_2$	36.87	5	|B' · B'|	1 550.2
$(310)_1/(130)_2$	53.13	5	|C'|	1 488.5

havior. Fig. 2(a) shows the |C| structure unit for the boundary of $\Sigma=5/(310)53.13°$ / [001], and the energy increase due to Mg atom substitution for Ni atom at different position (A, B, C or D) in |C| units. It can be seen that the energies for the substitution of Mg for Ni at A and D positions are $\Delta E^{A}_{segr}=-0.024$ eV and $\Delta E^{D}_{segr}=-1.5$ eV repectively, but the $\Delta E^{B}_{segr}=0.491\,5$ eV and $\Delta E^{C}_{segr}=0.427\,1$ eV, so it is stable and favorable that Mg atoms segregate to the D position. Similarly, it can be indicated from Fig. 2(b) , (c) and (d), that the B and C positions in |B| structure unit for the boundary of $\Sigma=5/(210)36.87°$ /[001] (Fig. 2(b)), the B position of |A| unit in |AB| structure of $\Sigma=13(320)22.62°$ /[001](Fig. 2(c)) , and the A position of first |A| unit of |AAAB'| structure of $\Sigma=41/(540)12.68°$ /[001] are the favorable segregation positions. The segregation energies are shown in Table 3.

Table 3 Segregation energies in various grain boundaries

Grain boundary	Position in unit	ΔE_{segr}/eV
Σ5/(310) 53.13 °/[001]	D in |C|	−1.5
Σ5/(210) 36.87 °/[001]	B in |B|	−0.68
	C in |B|	−0.64
ΣB/(320) 22.62 °/[001]	B in |A|	−1.286
ΣA/(540) 12.68 °/[001]	A in |A|	−1.338

Fig. 2(a) ~ (d) also show the calculated results in local stress tensor. It can be seen that the favorable segregation positons are always consistent with the positions at which the hydrostatic stressed approximate zero. Actually this is the position at which the local stress tensor changes from tension to compression. These positions, then can be defined as grain boundary dislocation cores.

Previous results undoubtedly attribute the Mg segregation to the equilibrium behavior which makes the grain boundary energy lower. Mg atoms which has larger atomic size segregate to grain boundary dislocation cores, leading a decrease in elastic strain energy. Since the segregation energy in |C| unit relatively large and the |C| unit is the frequent constituent for high-angle grain boundaries, the driving force of Mg segregation to high-angle train boundaries is the largest. Fig. 3 shows an experimental evidence to conform the equilibrium segregation behavior of Mg in Ni-based superalloys. Long times exposure at high temperature increases the degree of Mg segregation at grain boundary, and makes the segregation layer thinner. Our expermental study also indicated the heterogeneity of Mg segregation either at different grain boundaries or at different sections of a grain boundary . This phenomenon should be related to the difference in structure of grain boundary.

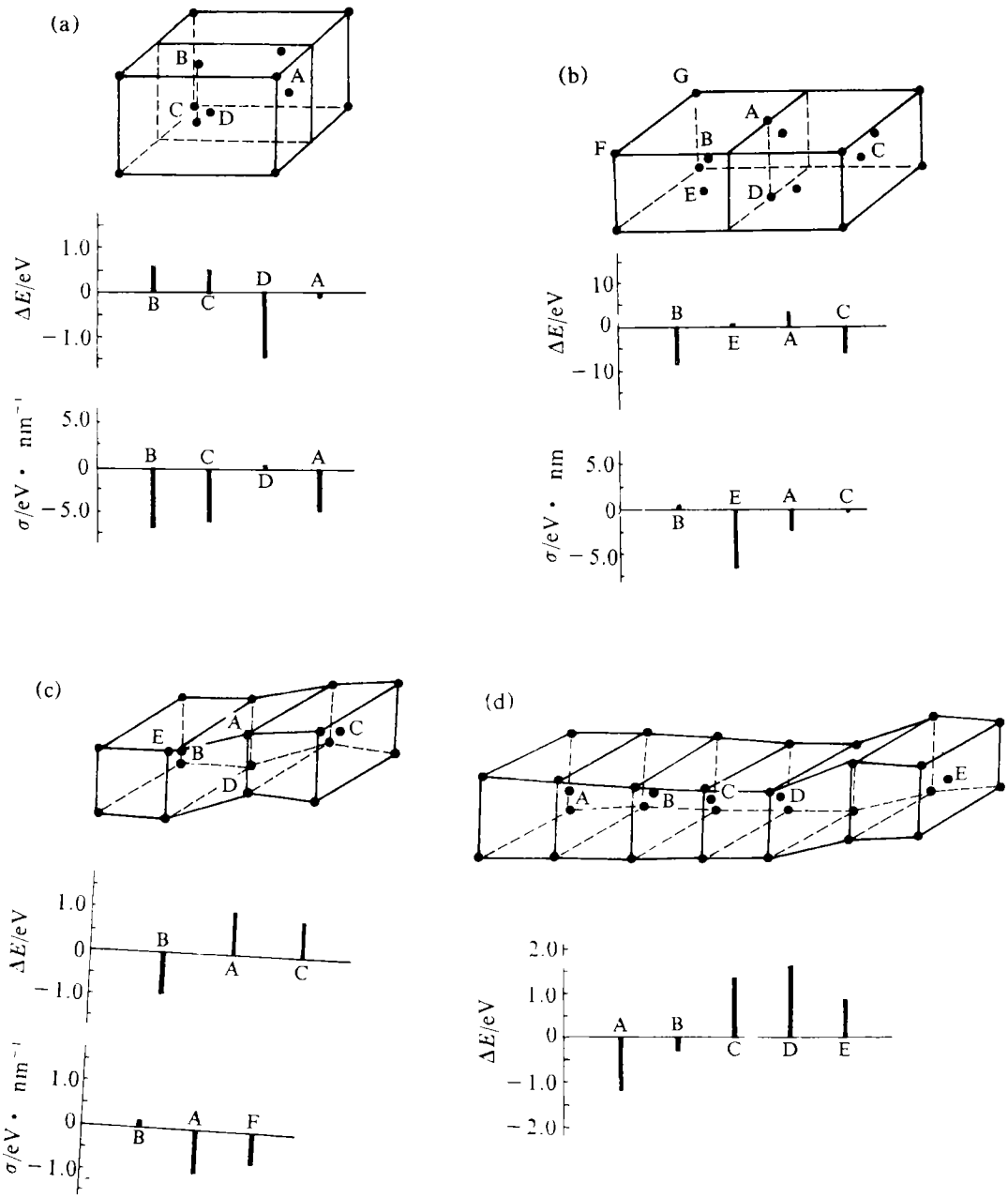

Fig. 4 Mg segregation energy ΔE and hydrostatic stress σ for various Mg atom sites

(a) in |C| structure of [100]/Σ5(310) grain boundary;

(b) in |BB′| structure of [100]/Σ5(210) grain boundary;

(c) in |AB′| structure of [100]/Σ13(320) grain boundary;

(d) in |AAAB′| structure of [100]/Σ41(540) grain boundary

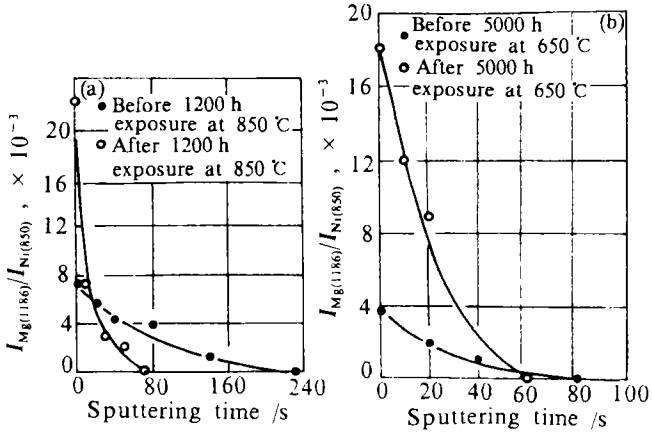

Fig . 3 Depth－Mg relative content profiles of GH220 with 0.019% Mg (a) and GH169 with 0.009 4%Mg (b) before and after long time exposure at high temperature

2.3 THE INFLUENCES OF Mg SEGREGATION ON BASIC GRAIN BOUNDARY BEHAVIOR

Fig. 4(a) and(b) show the influence of Mg segregation on the distribution of electronic density in structure unit.The instanced grain boundary is Σ5/(210), 36.87 °/[001]. Along two directions AB tie and FG tie in |B| structure unit, the distribution of electronic density was calculated. It can be seen that Mg segregation to B or/and C position in |B| unit increases the electronic density and makes its distribution more homogeneous.

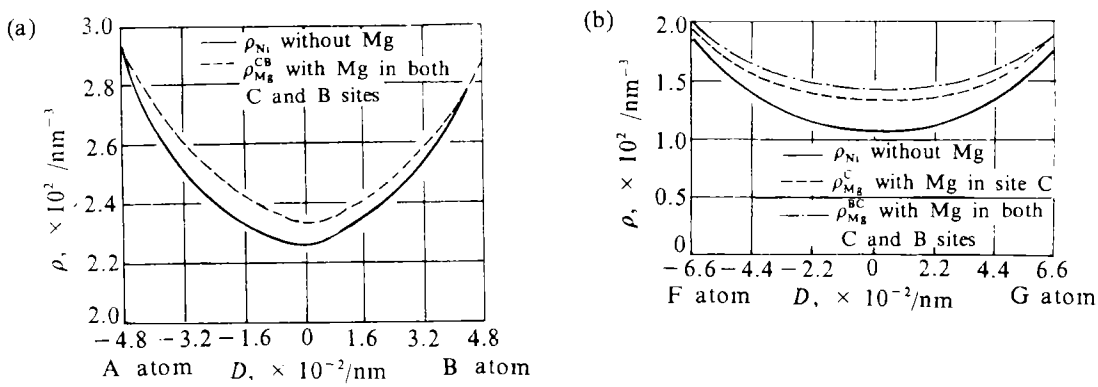

Fig. 4 The electron density distribution in [100]/Σ5(210) between A and D (a), and F and G (b) atoms |BB| structure

Fig. 5 shows the influence of Mg segregation on the vacancy formation energy. The Mg segregation at B position in |B| unit for the boundary of Σ5/(210), 36.87 °/[001] increases the vacancy formation energy. As the distance between segregated Mg atom and vacancy increases the increment of vacancy formation energy decreases. For instance, for the E vacancy which is the nearest the ΔE_v increases by 10%. For the F

vacancy which is far from segregated Mg atom the ΔE_v only increases by 2%. The reason for the increase in vacancy formation energy, we believe, lie on the increase in electronic density of background due to Mg segregation. The increased of background electronic density should decrease the embedding energy and increased the vacancy formation energy.

2.4 GRAIN BOUNDARY STRENGTHENING MECHANISMS OF Mg IN Ni-BASED SUPERALLOYS

Fig. 6 is a typical example to show the influence of Mg in instanced superally GH698 on creep behavior. Mg improves both creep life and elongation significantly due to the prolongation of the secondary creep stage and the development of tertiary creep stage, but has no evident influence on creep rate of the alloy. Fig. 7 is another example to prove that Mg addition in Ni-based superalloys reduces the creep growth rate. The fractographs of fracture surfaces show that Mg addition changes a brittle intergranular fracture to a ductile intergranular fracture. All these results obwiously indicate that the Mg addition strengthens the grain boundaries mainly due to the retardation in intergranular void initiation and the decrease in creep crack growth rate. The results of the computer simulation have proved that the beneficial effects of Mg addition on grain boundaries are related to the grain boundary segregation behavior and its influence on the grain boundary properties. The main mechanisms include:

(1) Grain boundary equilibrium segregation behavior of Mg.

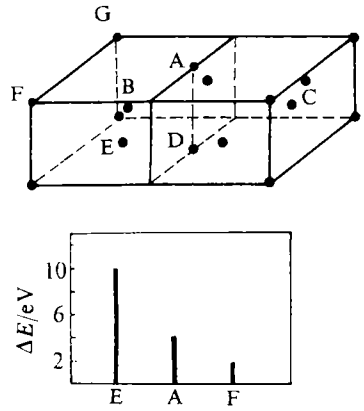

Fig. 5 The influence of Mg segregation at atom site B boundary on formation energy of a vacancy in atom sites E, A, and F for [100]/Σ5(210) grain boundary respectively

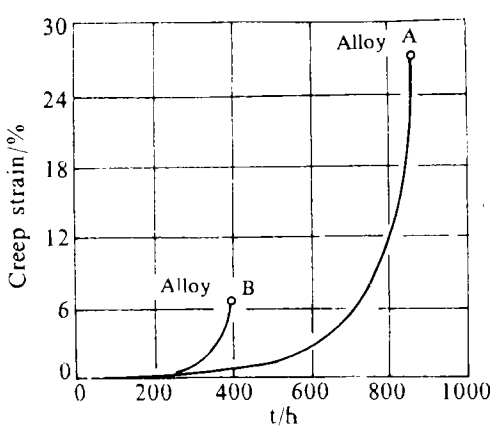

Fig. 6 Creep curves of alloy A (containing 0.005%Mg) and B (no Mg) at 750 ℃ and 343 MPa

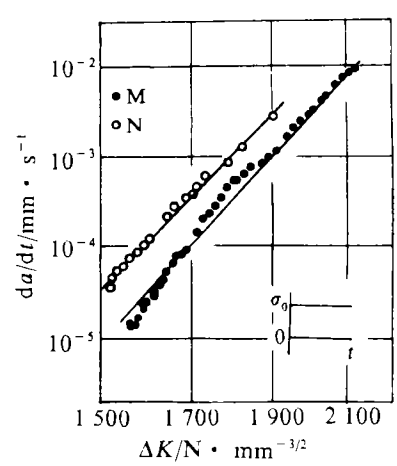

Fig. 7 Crack growth rate of GH33A with Mg (M) and without Mg (N)

(2) Grain boundary cohesive bond is intensified in terms of the increase and more homogeneous distribution in electronic density due to Mg segregation.

(3) The decrease in mobility of the grain boundary dislocations due to Mg atom segregation to dislocation cores. It may influence the creep rate if the grain boundary creep predominates over the creep in grain.

(4) Mg segregation increases the vacancy formation energy, and results in the decreases in grain boundary vacancy concentration and grain boundary diffusion coefficient.

(5) The morphology of grain boundary precipitates may be changed due to the decrease in grain boundary energy, the uniform granular grain boundary precipitates decreased the mobility of grain boundary migration, and results in the retardation of creep voids initiation and growth.

3 CONCLUSIONS

The computer simulation of Mg segregation to grain boundary in Ni offers a better understanding in the strengthening mechanism of Mg additiion in Ni－based superalloys . Small amount of Mg addition in Ni－based superalloys offer a great improvements in creep related properties due to Mg grain boundary segregation retarding the creep voids initiation and growth.

REFERENCES

1 Xu Z, Ma P. The effect and control of trace elements in superalloys. Beijing : Metallurgical Press. 1987. (in Chinese)
2 Chen G, Wang D, Xu Z, Xie X, et al. In: Gell M, et al, eds. Proceedings of Superalloys 1984. AIME, 1984 . 611
3 Chen G, Zhang T, Yang W. High Temperature Technology. 1988, 6(3) : 149
4 Xie X, Xu Z, et al . In: Duhl D N, et al. eds. Proceedings of Superalloys 1988. AIME, 1988. 635
5 Foiles S M, Baskes M I, et al Phys Rev B. 1986, 33(3) : 7983
6 Pusko M J, Nieminen R M, et al . Phys Rev B, 1981, 24(6) : 3037
7 Tewordt L , et al. Phys Rev, 1958, 109 ; 61
8 Sutton A P, et al. Acta Metall, 1982, 30 : 2011
9 Sutton A P, et al . Scripta Metall. 1980, 14 : 129
10 Sutton A P , Vitek V. Phil Trans R Soc Lond, 1983, A309 : 1
11 Murr L E. Interfacial Phenomenal in Metals and Alloys . New York : Addison－Wesley, 1975, 132

(To page 108)

电沉积 Cr_2O_3 氧化膜对 Fe_3Al 氧化性能的影响

王永刚 何业东 朱日彰
北京科技大学表面科学与腐蚀工程系，北京 100083

摘要 通过电沉积－反应烧结方法在 Fe_3Al 表面制得了均匀致密无鼓泡等缺陷的 Cr_2O_3 薄膜，这种薄膜在室温下呈非晶态．本文用 TEM, EDAX, SEM 和 XRD 等手段研究了这种薄膜对 Fe_3Al 在 900 ℃ 空气中氧化行为的影响，发现表面沉积这种薄膜可以使氧化层晶粒细化并促进 Al 的选择性氧化，从而提高了 Fe_3Al 的抗高温氧化性能．

关键词 氧化，Fe_3Al，薄膜

(From page 91)

Mg 在 Ni 基高温合金中的晶界偏析行为和强化机制的计算机模拟

陈国良[1)] 葛红林[1)]
北京科技大学新金属国家重点实验室，北京 100083

摘要 用嵌入原子势函数和静态弛豫方法模拟了镁在高温合金中的晶界偏析行为．模拟结果指出，Mg 确有晶界平衡偏析行为．Mg 的晶界偏析使晶界区电子密度分布更加均匀，提高晶界结合强度和空位形成能，减少晶界位错可动性，因此推迟蠕变孔洞的形成和长大，这是 Mg 的主要强化机制．

关键词 高温合金中的 Mg，晶界偏析，高温合金，计算机晶界偏析摸拟